

## NiO films consisting of vertically aligned cone-shaped NiO rods

Zhengjun Zhang, Ye Zhao, and Minmin Zhu

Citation: *Applied Physics Letters* **88**, 033101 (2006); doi: 10.1063/1.2166479

View online: <http://dx.doi.org/10.1063/1.2166479>

View Table of Contents: <http://scitation.aip.org/content/aip/journal/apl/88/3?ver=pdfcov>

Published by the [AIP Publishing](#)

---

### Articles you may be interested in

[Effect of Cu doping on the resistive switching of NiO thin films](#)

*J. Appl. Phys.* **115**, 164507 (2014); 10.1063/1.4873455

[Strong energy-transfer-induced enhancement of Er<sup>3+</sup> luminescence in In<sub>2</sub>O<sub>3</sub> nanocrystal codoped silica films](#)

*Appl. Phys. Lett.* **103**, 181906 (2013); 10.1063/1.4827883

[Transformation from an atomically stepped NiO thin film to a nanotape structure: A kinetic study using x-ray diffraction](#)

*Appl. Phys. Lett.* **93**, 241904 (2008); 10.1063/1.3050112

[Field emission properties of ZnO nanorods coated with NiO film](#)

*J. Vac. Sci. Technol. B* **26**, 1021 (2008); 10.1116/1.2919156

[Reproducible resistance switching in polycrystalline NiO films](#)

*Appl. Phys. Lett.* **85**, 5655 (2004); 10.1063/1.1831560

---

The advertisement features a row of computer monitors in a library setting, each displaying the cover of the journal 'Computing: Science & Engineering'. The covers show a colorful, abstract pattern. In the bottom right corner, the journal's logo is displayed in orange and black. Below the monitors, the text 'AIP's JOURNAL OF COMPUTATIONAL TOOLS AND METHODS. AVAILABLE AT MOST LIBRARIES.' is written in white and yellow on a dark background.

**computing**  
SCIENCE & ENGINEERING

AIP's JOURNAL OF COMPUTATIONAL TOOLS AND METHODS.  
**AVAILABLE AT MOST LIBRARIES.**

## NiO films consisting of vertically aligned cone-shaped NiO rods

Zhengjun Zhang,<sup>a)</sup> Ye Zhao, and Minmin Zhu

Advanced Materials Laboratory, Department of Materials Science and Engineering, Tsinghua University, Beijing 100084, People's Republic of China

(Received 28 July 2005; accepted 18 November 2005; published online 18 January 2006)

By thermally heating a nickel foil in a vacuum of  $\sim 5 \times 10^{-2}$  Torr, films consisting of vertically aligned cone-shaped NiO microrods were deposited on Si (001) substrates at a temperature of  $< 300$  °C. The NiO rods were grown along  $\langle 001 \rangle$  directions by stacking the NiO (001) nanoslices, and are  $\sim 10$   $\mu\text{m}$  long with a sharp nanosized tip. Due to this morphology, the NiO film exhibited a threshold field of  $\sim 6.5$  V/ $\mu\text{m}$  in field emission and a field enhancement factor of 2130 that is sufficiently high for field emission applications. The optical band gap of the NiO film was estimated to be  $\sim 3.68$  eV from the optical absorption measurement and was almost a constant upon heating. In addition, the NiO film exhibited a strong photoluminescence at  $\sim 674$  nm when excited by a 514 nm Ar<sup>+</sup> laser, which might be attributed to the oxygen vacancies. © 2006 American Institute of Physics. [DOI: 10.1063/1.2166479]

There has been increasing interest in developing nanostructures of metal oxides due to their outstanding properties and potential applications in electronic and optoelectronic devices.<sup>1,2</sup> Among the transition metal oxides, nickel oxide has attracted considerable attention in recent years because of its wide band gap and excellent dielectric properties,<sup>3</sup> for example, NiO demonstrated a giant dielectric constant when doped with lithium,<sup>4</sup> and has thus been widely studied for applications in electrochromic display devices,<sup>5</sup> gas sensors,<sup>6</sup> *p*-type transparent conducting electrodes,<sup>7</sup> thermoelectric devices,<sup>8</sup> magnetoresistance sensors,<sup>9</sup> etc. However, there are few studies on the optical and field emission properties of NiO, especially for NiO nanostructures. Thus, it is of great interest to synthesize and investigate the related properties of NiO nanostructures.

To date, NiO nanostructures have been mostly synthesized by the hydrothermal method.<sup>10–13</sup> For example, Lin and co-workers<sup>12</sup> produced aligned polycrystalline NiO nanowires using a hydrothermal method with anodic alumina membranes as templates; NiO nanowires have been synthesized by heating Ni(OH)<sub>2</sub> nanorods in a muffle furnace at 500 °C.<sup>13</sup> Although the hydrothermal method is a powerful technique in synthesizing metal oxides nanostructure, it is very hard to fabricate arrays of aligned nanostructures on flat substrates, such as silicon, which is a necessity for device applications.<sup>14</sup> Therefore, new methodologies that are simple and capable of producing metal oxides nanostructures on planar substrates are highly demanded.

In this study, we employed a thermal oxidation method to synthesize nanostructures of NiO. By this means, NiO films consisting of vertically aligned cone-shaped NiO rods were deposited on silicon substrates. The NiO rods were several  $\mu\text{m}$  long and submicron in diameter and had a sharp nanosized tip; thus resulting in a large field enhancement factor for field emission. The optical properties of the NiO films were also studied.

The nickel oxide nanostructures were prepared using a simple thermal oxidization approach described in our

pervious works.<sup>15,16</sup> By heating a nickel foil (50 mm $\times$ 5 mm $\times$ 0.6 mm) in a vacuum of  $5 \times 10^{-2}$  Torr, NiO films were deposited on Si substrates  $\sim 2$  cm above the nickel foil. Within a typical deposition time of 20 min, the temperature of the Si substrates was measured to be below 300 °C by a K-type thermocouple. The advantage of this approach is the easy control of the nanostructures growth via adjusting the pressure and the current passing the foil. The growth morphology, phase structure, and related properties of the deposits were examined by scanning electron microscopy (SEM), transmission electron microscopy (TEM), x-ray diffraction (XRD), Raman spectrometer, optical absorption measurement, and field emission measurement, respectively.

By passing a current of  $\sim 60$ A through the nickel foil (the temperature of the nickel foil was measured to be  $\sim 1250$  °C) in a vacuum of  $\sim 5 \times 10^{-2}$  Torr for 20 min, a thin NiO film was deposited on silicon substrates. Figures 1(a) and 1(b) show the XRD pattern and Raman spectrum of the deposits, respectively. The XRD pattern was taken with a Rigaku x-ray diffractometer using the Cu  $K\alpha$  radiation. The XRD pattern clearly shows the diffraction peaks of (111), (200), (220), (311), and (222) of the face-centered-cubic (fcc) structured NiO at  $2\theta = 37.27^\circ$ ,  $43.30^\circ$ ,  $62.90^\circ$ ,  $75.44^\circ$ , and  $79.43^\circ$ , respectively.<sup>17</sup> The Raman spectrum was taken with a Reinsaw 1000 micro-Raman spectrometer using a 325 nm He–Cd laser as the excitation source. It shows strong Raman peaks at 559, 721, 891, 1093, and 1429  $\text{cm}^{-1}$  in the range of 500–1500  $\text{cm}^{-1}$ ; both the position and relative intensity of the peaks are in good agreement with that reported for NiO with a fcc structure.<sup>18</sup> These suggest that NiO films with a fcc structure were deposited on the silicon substrates by this simple thermal oxidation method.

Figures 2(a)–2(d) show SEM images of the growth morphology of the NiO film. The SEM images were taken with a LEO-6301 SEM working at 20 kV. The NiO film, as seen from Fig. 2(a), consisted of densely packed vertically aligned NiO rods with a length of  $\sim 10$   $\mu\text{m}$ . The rods are normally submicron in diameter and are of nano size (several tens nm) cone-shaped flat tip, see arrows in Fig. 2(d). It can also be seen from Fig. 2(d) that the NiO rods were formed by stacking of parallel NiO nanoslices along the growth direction.

<sup>a)</sup> Author to whom correspondence should be addressed; electronic mail: zjzhang@tsinghua.edu.cn

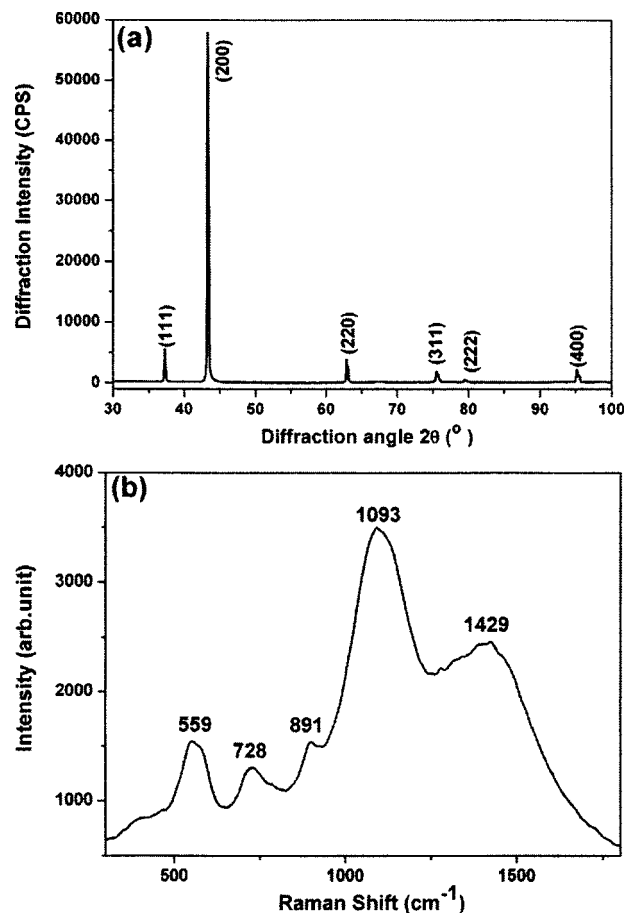


FIG. 1. (a) XRD pattern and (b) Raman spectrum of the NiO film deposited on a Si (001) substrate.

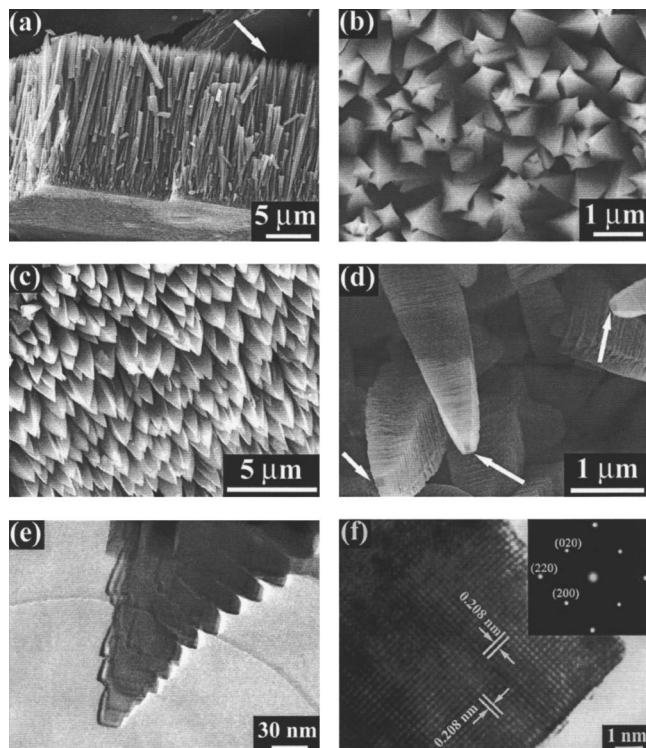


FIG. 2. (a) A side-view of the NiO film consisting of vertically aligned NiO microrods; (b) and (c) are a top view and a tilt view of the sharp tips of the NiO microrods indicated by the arrow in (a); (d) is a high magnification SEM image of the flat top of the sharp tips of NiO microrods (see arrows); (e) and (f) are TEM and HRTEM images of the sharp tip of the NiO microrods respectively. Inset of (f) is a corresponding SAD pattern of the tip.

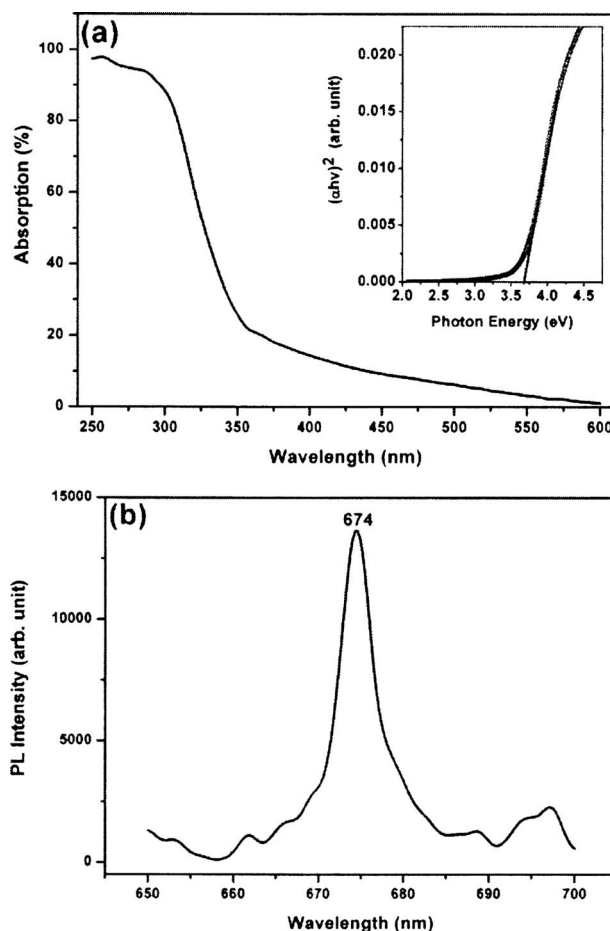


FIG. 3. (a) A typical optical absorption spectrum of the NiO film, inset is a plot at the absorption edge; and (b) a typical room-temperature photoluminescence spectrum of the NiO film excited with a 514 nm Ar<sup>+</sup> laser.

Figures 2(e) and 2(f) are the TEM, high-resolution TEM (HRTEM) and corresponding selective area diffraction (SAD) pattern of an individual NiO rod, taken with a JEM-2010F TEM working at 200 kV. It shows that the NiO rod is single crystalline, and was grown along the  $\langle 200 \rangle$  direction by stacking NiO (200) slices with a thickness of several tens nm. This is why the NiO film shows a  $\langle 200 \rangle$  fabric texture in the XRD pattern [see Fig. 1(a)].

Figure 3(a) shows a typical optical absorption spectrum of the NiO film measured with a UV2100 spectrophotometer at room temperature. The inset is a plot of the absorption edge, from which the optical band gap ( $E_g$ ) of the NiO film can be derived using;  $(\alpha h\nu)^2 = A(h\nu - E_g)$ , where  $\alpha$  is the absorption coefficient,  $E_g$  is the optical band gap,  $A$  is the edge-width parameter, and  $h\nu$  is the photon energy, respectively.<sup>19–21</sup> From the inset, the optical band gap of the NiO film was estimated to be 3.68 eV, which is in agreement with the data reported in the literature.<sup>12,22,23</sup> The optical band gap of the NiO film was very stable upon heating in the air. For example, the  $E_g$  value changed from 3.68 to 3.62 eV after annealing at a temperature of 650 °C, which is only a 1.6 % decrease. Figure 3(b) shows a typical photoluminescence spectrum of the NiO film excited by a 514 nm Ar<sup>+</sup> laser at room temperature. It clearly shows a strong emission at  $\sim 674$  nm. This emission could be probably due to the oxygen vacancies in the NiO rods, which could result from the current deposition method, i.e., NiO rods were grown in a vacuum environment of limited oxygen supply.

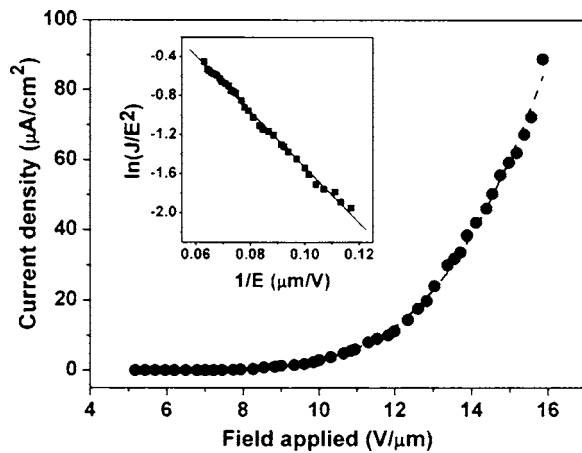


FIG. 4. The room-temperature field emission of the NiO film. Inset is the F-N plot of the field emission curve.

Since the NiO film synthesized by this deposition method consist of vertically aligned NiO rods with sharp nanosized tips, see Figs. 2(a)–2(d), the NiO film might have good field emission properties. The field emission of the NiO film was thus measured with a Keithley 485 electrometer in chamber with a vacuum level of  $6 \times 10^{-9}$  Torr at room temperature. In measurement, the area of the sample was  $0.5 \text{ cm}^2$  and the separation between two electrodes was  $250 \text{ }\mu\text{m}$ . Figure 4 shows a typical field emission curve of the NiO film. The threshold field of the NiO film (defined as the field to obtain a current density of  $0.1 \text{ }\mu\text{A}/\text{cm}^2$ ) was found to be  $\sim 6.5 \text{ V}/\mu\text{m}$ , and the turn-on field of the NiO film (defined as the field to obtain a current density of  $10 \text{ }\mu\text{A}/\text{cm}^2$ ) was estimated to be  $11.5 \text{ V}/\mu\text{m}$ , which are similar to that of the  $\text{Cu}_2\text{S}$  and  $\text{ZnO}$  nanowires.<sup>24,25</sup> The field emission behavior of the NiO film can be explained well with the Fowler–Nordheim (F-N) theory of  $J = (E^2 \beta^2 / \phi) \exp(-B \phi^{3/2} / E \beta)$ , where  $J$  is the current density,  $E$  is the field applied ( $E = V/d$ ),  $\phi$  is the work function of the materials,  $\beta$  is the field-enhancing factor, and  $B = 6.83 \times 10^9 (\text{eV}^{-3/2} \mu\text{m}^{-1})$ .<sup>26</sup> Inset of Fig. 4 is the F-N plot. The perfect linearity of the  $\ln(J/E^2)$  versus  $1/E$  curve indicated that the field emission of the NiO film matches well with the F-N theory. Using the work function of 4.3 eV for NiO, the field enhancement factor  $\beta$  of this NiO film was

estimated to be  $\sim 2130$ , which is sufficiently high for field emission applications.

In summary, by thermal oxidizing a thin nickel foil in a low vacuum, NiO films consisting of vertically aligned NiO rods of cone-shaped nanosized tips were deposited on flat substrates, at a temperature below  $300 \text{ }^\circ\text{C}$ . The film was of an optical band gap of  $\sim 3.68 \text{ eV}$  that was quite stable upon heating in the air, and exhibited room-temperature photoluminescence at  $\sim 674 \text{ nm}$ . Due to the special growth morphology of the NiO film, it showed a field enhancement factor of  $\sim 2310$ , which is sufficiently high for field emission applications.

The authors are grateful to the financial support of NSFc (Grant No. 50225102), and the partial support from the Ministry of Science and Technology of China.

- <sup>1</sup>M. H. Huang, S. Mao, and H. Feick, *Science* **292**, 1897 (2001).
- <sup>2</sup>Z. W. Pan, Z. R. Dai, and Z. L. Wang, *Science* **291**, 1947 (2001).
- <sup>3</sup>H. Sato, T. Minami, S. Takata, and T. Yamada, *Thin Solid Films* **236**, 27 (1993).
- <sup>4</sup>J. B. Wu, C.-W. Nan, Y. H. Lin, and Y. Deng, *Phys. Rev. Lett.* **89**, 217601 (2002).
- <sup>5</sup>M. Kitao, K. Izawa, and K. Urabe, *Jpn. J. Appl. Phys., Part 1* **33**, 6656 (1994).
- <sup>6</sup>I. Hotovy, J. Huran, and P. Siciliano, *Sens. Actuators B* **78**, 126 (2001).
- <sup>7</sup>I. M. Chan, T. Y. Hsu, and F. C. Hong, *Appl. Phys. Lett.* **81**, 1899 (2002).
- <sup>8</sup>W. Shin and N. Murayama, *Mater. Lett.* **45**, 302 (2000).
- <sup>9</sup>M. J. Carey and A. E. Berkowitz, *J. Appl. Phys.* **73**, 6892 (1993).
- <sup>10</sup>J. Qi, T. Zhang, and M. Lu, *Chem. Lett.* **34**, 180 (2005).
- <sup>11</sup>X. Wang, J. M. Song, and L. S. Gao, *Nanotechnology* **16**, 37 (2005).
- <sup>12</sup>Y. Lin, T. Xie, B. C. Cheng, B. Y. Geng, and L. D. Zhang, *Chem. Phys. Lett.* **380**, 521 (2003).
- <sup>13</sup>J. H. Liang and Y. D. Li, *Chem. Lett.* **32**, 1126 (2003).
- <sup>14</sup>Y. N. Xia, P. D. Yang, and Y. G. Sun, *Adv. Mater. (Weinheim, Ger.)* **15**, 353 (2003).
- <sup>15</sup>J. G. Liu, Z. J. Zhang, and Y. Zhao, *Small* **1**, 310 (2005).
- <sup>16</sup>J. G. Liu, Z. J. Zhang, and C. Y. Pan, *Mater. Lett.* **58**, 3812 (2004).
- <sup>17</sup>JCPDS Card: 47-1049.
- <sup>18</sup>R. E. Dietz, G. I. Parisot, and A. E. Meixner, *Phys. Rev. B* **4**, 2302 (1971).
- <sup>19</sup>D. Adler and J. Feinlieb, *Phys. Rev. B* **2**, 3112 (1970).
- <sup>20</sup>P. S. Patil and L. D. Kadam, *Appl. Surf. Sci.* **199**, 211 (2002).
- <sup>21</sup>T. Toyoda, H. Nakanishi, S. Endo, and T. Irie, *J. Phys. D* **18**, 747 (1985).
- <sup>22</sup>D. Adler and J. Feinlieb, *Phys. Rev. B* **2**, 3112 (1970).
- <sup>23</sup>A. B. Kunz, *J. Phys. C* **14L**, 445 (1981).
- <sup>24</sup>J. Chen, S. Z. Deng, and N. S. Xu, *Appl. Phys. Lett.* **80**, 3620 (2002).
- <sup>25</sup>C. J. Lee, T. J. Lee, and S. C. Lyu, *Appl. Phys. Lett.* **81**, 3648 (2002).
- <sup>26</sup>R. H. Fowler and L. W. Nordheim, *Proc. R. Soc. London, Ser. A* **119**, 173 (1928).